

## Excited-State Electron Transfer in a Chromophore–Quencher Complex. Spectroscopic Identification of a Redox-Separated State

Rosa López,<sup>†</sup> Ana M. Leiva, Fernando Zuloaga, and Bárbara Loeb\*

Facultad de Química, P. Universidad Católica de Chile, Vicuña Mackenna 4860, Santiago, Chile

Ester Norambuena

Departamento de Química, Facultad de Ciencias Básicas, Universidad Metropolitana de Ciencias de la Educación, Casilla 147, Santiago, Chile

Kristin M. Omberg, Jon R. Schoonover,<sup>‡</sup> Durwin Striplin,<sup>§</sup> Martin Devenney, and Thomas J. Meyer\*

Department of Chemistry, CB#3290, University of North Carolina, Chapel Hill, North Carolina 27599-3290

Received September 1, 1998

In the chromophore–quencher complex *fac*-[Re(Aqphen)(CO)<sub>3</sub>(py-PTZ)]<sup>+</sup> (Aqphen is 12,17-dihydronaphtho[2,3-h]dipyrido[3,2-a:2',3'-c]-phenazine-12,17-dione; py-PTZ is 10-(4-picolyl)phenothiazine), Aqphen is a dppz derivative, containing a pendant quinone acceptor at the terminus of a rigid ligand framework. This introduces a third, low-lying, ligand-based  $\pi^*$  acceptor level localized largely on the quinone fragment. Laser flash excitation of *fac*-[Re(Aqphen)(CO)<sub>3</sub>(py-PTZ)]<sup>+</sup> (354.7 nm; in 1,2-dichloroethane) results in the appearance of a relatively long-lived transient that decays with  $\tau_{298K} = 300$  ns ( $k = 3.3 \times 10^6$  s<sup>-1</sup>). Application of transient absorption, time-resolved resonance Raman, and time-resolved infrared spectroscopies proves that this transient is the redox-separated state *fac*-[Re<sup>I</sup>(Aqphen<sup>-</sup>)(CO)<sub>3</sub>(py-PTZ<sup>+</sup>)]<sup>+</sup> in which the excited electron is localized largely on the quinone portion of the Aqphen ligand.

### Introduction

The acceptor ligand dppz (dipyrido[3,2-a:2',3'-c]phenazine) has two low-lying  $\pi^*$  acceptor levels, one localized primarily on the phenanthroline portion of the ligand and one on the phenazine portion. The energy ordering is  $\pi^*$ (phenanthroline) >  $\pi^*$ (phenazine), and in complexes, such as [Ru(bpy)<sub>2</sub>(dppz)]<sup>2+</sup> (bpy is 2,2'-bipyridine), metal-to-ligand charge transfer (MLCT) excitation to the phenanthroline-based  $\pi^*$  level is followed by rapid, internal electron transfer to the emissive, phenazine-based level.<sup>1–4</sup> On the basis of the relative absorptivities of the associated MLCT bands, the phenanthroline-based level is more strongly coupled to the metal center than the phenazine-based level.

We report herein the first photophysical studies on Re complexes, containing the dppz derivative Aqphen (Aqphen is

12,17-dihydronaphtho[2,3-h]dipyrido[3,2-a:2',3'-c]-phenazine-12,17-dione), which contains a pendant quinone acceptor at the terminus of the rigid dppz ligand framework.<sup>5</sup> Quinone acceptors are used widely in studies of photoinduced electron and energy transfer,<sup>6–11</sup> and the quinone fragment in Aqphen introduces a third, even lower-lying, ligand-based  $\pi^*$  acceptor level, localized largely on the quinone. Time-resolved infrared (TRIR) measurements on the chromophore–quencher complex, *fac*-[Re(Aqphen)(CO)<sub>3</sub>(py-PTZ)]<sup>+</sup> (**1**, py-PTZ is 10-(4-picolyl)phenothiazine), following Re<sup>I</sup> → Aqphen excitation clearly demonstrate that the excited electron is ultimately localized on the quinone part of the ligand, as the acceptor in a redox-separated state.

### Experimental Section

**Materials.** All chemicals were reagent grade and used as received unless otherwise specified. Re(CO)<sub>5</sub>Cl was kindly supplied by Dr. H.

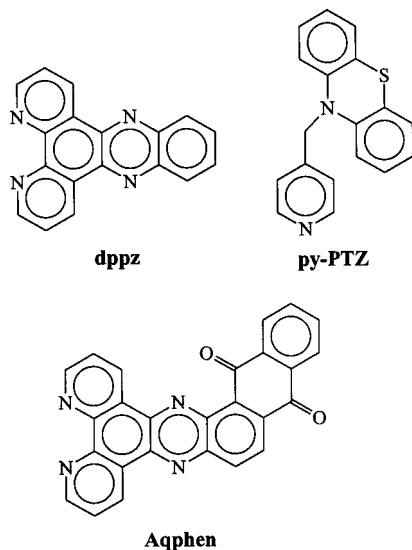
<sup>†</sup> Current address: Wichita State University, Wichita, KS.

<sup>‡</sup> Present address: Bioscience and Biotechnology Group (CST-4), Chemical Science and Technology Division, Mail Stop J586, Los Alamos National Laboratory, Los Alamos, NM 87545.

<sup>§</sup> Present address: Department of Chemistry, Martin Chemistry Laboratory, Davidson College, Davidson, NC 28036.

- (1) Olson, E. J. C.; Hu, D.; Hörmann, A.; Jonkman, A. M.; Arkin, M. R.; Stemp, E. D. A.; Barton, J. K.; Barbara, P. F. *J. Am. Chem. Soc.* **1997**, *119*, 11458.
- (2) Schoonover, J. R.; Bates, W. D.; Strouse, G. F.; Chen, P.; Dyer, R. B.; Meyer, T. J. *Inorg. Chem.* **1995**, *35*, 473.
- (3) Friedman, A. E.; Chambron, J. C.; Sauvage, J. P.; Turro, N. J.; Barton, J. K. *J. Am. Chem. Soc.* **1990**, *112*, 4960–4962.
- (4) Amouyal, E.; Homsí, A.; Chambron, J. C.; Sauvage, J. P. *J. Chem. Soc., Dalton Trans.* **1990**, 1841–1845.

- (5) López, R.; Loeb, B.; Boussie, T.; Meyer, T. J. *Tetrahedron Lett.* **1996**, *37*, 5437.
- (6) Kuciauskas, D.; Liddell, P. A.; Gust, D. *J. Phys. Chem. B* **1997**, *101*, 429.
- (7) Kurreck, H.; Huber, M. *Angew. Chem.* **1995**, *34*, 849–866.
- (8) Macpherson, A. N.; Liddell, P. A.; Gust, D. *J. Am. Chem. Soc.* **1995**, *117*, 7202.
- (9) Mecklenburg, S. L.; McCafferty, D. G.; Schoonover, J. R.; Peek, B. M.; Erickson, B. W.; Meyer, T. J. *Inorg. Chem.* **1994**, *33*, 2974–2983.
- (10) Opperman, K. A.; Mecklenburg, S. L.; Meyer, T. J. *Inorg. Chem.* **1994**, *33*, 5295–5301.
- (11) Wasielewski, M. R. *Chem. Rev.* **1992**, *92*, 435.



Klahn from the Universidad Católica de Valparaíso.<sup>12</sup> Tetrahydrofuran, acetonitrile, anhydrous methanol, diethyl ether, ethanol,  $\text{NH}_4\text{PF}_6$ , petroleum ether, 1,2-dichloroethane, 4-ethylpyridine (4-Etpy), phenothiazine (PTZ), dichloromethane, silver trifluoromethanesulfonate ( $\text{AgOTf}$ ), potassium *tert*-butoxide, DMSO, chloroform, and chloroform-*d* were purchased from Aldrich. 1,2-Dichloroethane was distilled from  $\text{CaH}_2$  before use.

**Syntheses.** The ligand Aqphen and *fac*-[Re(Aqphen)(CO)<sub>3</sub>Cl] were prepared as described in a previous communication.<sup>5</sup> 10-(4-Picolyl)-phenothiazine (py-PTZ) was prepared according to a literature procedure.<sup>13,14</sup> The complexes *fac*-[Re(Aqphen)(CO)<sub>3</sub>(OTf)], *fac*-[Re(Aqphen)(CO)<sub>3</sub>(4-Etpy)]( $\text{PF}_6$ ), and *fac*-[Re(Aqphen)(CO)<sub>3</sub>(py-PTZ)]( $\text{PF}_6$ ) (OTf is trifluoromethanesulfonate; 4-Etpy is 4-ethylpyridine) were prepared by a variation of the literature procedures for their bpy analogues,<sup>14,15</sup> as described below.

***fac*-[Re(Aqphen)(CO)<sub>3</sub>(OTf)].** *fac*-[Re(Aqphen)(CO)<sub>3</sub>Cl] (306 mg, 0.426 mmol) and  $\text{AgOTf}$  (109 mg, 0.426 mmol) were suspended in 25 mL of THF. The mixture was heated at reflux for 1 h under an inert atmosphere in the dark, then cooled to room temperature. The solution was filtered to remove  $\text{AgCl}$ , and the filtrate was evaporated to dryness. The resulting yellow solid was dissolved in acetonitrile, and the product precipitated by addition of diethyl ether. The solid was isolated by vacuum filtration, washed with copious quantities of ether, and purified by column chromatography on alumina with 10:1 (v/v) acetonitrile/ethanol as eluent. Yield, 270 mg (76.2%). Anal. Calcd for  $\text{ReC}_{30}\text{H}_{12}\text{N}_4\text{SO}_6\text{F}_3$ : C, 43.11; H, 1.94, Found: C, 43.32; H, 1.45.

***fac*-[Re(Aqphen)(CO)<sub>3</sub>(4-Etpy)]( $\text{PF}_6$ ).** *fac*-[Re(Aqphen)(CO)<sub>3</sub>(OTf)] (120 mg, 0.144 mmol) and excess 4-ethylpyridine (0.1 mL) were combined in 30 mL of anhydrous methanol. The mixture was heated at reflux for 3 h under an inert atmosphere. The solution was cooled to room temperature, and an excess of  $\text{NH}_4\text{PF}_6$  was added as a saturated solution in methanol. The mixture was stirred for 1 h, during which a yellow precipitate formed. After the mixture was placed in the refrigerator for 12 h, the methanol was removed by decantation. The precipitate was obtained by vacuum filtration, washed with copious quantities of petroleum ether, and purified on an alumina column with petroleum ether and then chloroform as eluent. The solution was concentrated by rotary evaporation, and the resulting product precipitated with diethyl ether, filtered, and then dried under high vacuum. Yield: 80 mg (70%). <sup>1</sup>H NMR ( $\text{CDCl}_3$ , ppm):  $\delta$  10.19 (dd, 1H),  $\delta$  10.02 (dd, 1H),  $\delta$  9.66 (dd, 2H),  $\delta$  8.87 (quart, 2H),  $\delta$  8.34 (m, 4H),  $\delta$

8.14 (d, 1H),  $\delta$  7.91 (m, 2H),  $\delta$  7.12 (d, 1H),  $\delta$  2.52 (quart, 2H),  $\delta$  1.05 (t, 3H).

***fac*-[Re(Aqphen)(CO)<sub>3</sub>(py-PTZ)]( $\text{PF}_6$ ).** *fac*-[Re(Aqphen)(CO)<sub>3</sub>(OTf)] (120 mg, 0.144 mmol) and py-PTZ (80 mg, 310  $\mu\text{mol}$ ) were dissolved in 30 mL of anhydrous methanol. The mixture was heated at reflux for 2 h under an inert atmosphere in the dark. The solution was cooled to room temperature, and an excess of  $\text{NH}_4\text{PF}_6$  was added as a saturated solution in methanol. The mixture was stirred for 12 h, resulting in the formation of a greenish-yellow precipitate. The methanol was removed by decantation. The precipitate was obtained by vacuum filtration, washed with copious quantities of petroleum ether, and purified on an alumina column with petroleum ether then 10:1 (v/v) dichloromethane/acetonitrile as eluent. The solution was concentrated by rotary evaporation, and the product was precipitated with diethyl ether then dried under high vacuum. Yield: 60.0 mg (37.2%). <sup>1</sup>H NMR ( $\text{CDCl}_3$ , ppm):  $\delta$  9.70 (m, 4H),  $\delta$  8.53 (quart, 2H),  $\delta$  8.33 (d, 1H),  $\delta$  8.24 (m, 2H),  $\delta$  8.04 (m, 2H),  $\delta$  7.82 (m, 2H),  $\delta$  7.28 (d, 1H),  $\delta$  6.91 (dd, 2H),  $\delta$  6.67 (dd, 4H),  $\delta$  6.43 (dd, 2H),  $\delta$  4.96 (s, 2H). Anal. Calcd for  $\text{ReC}_{47}\text{H}_{30}\text{N}_6\text{SO}_3$ : C, 50.58; H, 2.34; N, 7.52. Found: C, 48.1; H, 2.6; N, 7.69.

**Measurements.** UV-visible spectra were recorded on Milton Roy 3000 or Hewlett-Packard 9452A diode array spectrometers. <sup>1</sup>H NMR spectra were recorded on a Bruker AC/200 200 MHz spectrometer with TMS as reference. Ground-state IR spectra were recorded as KBr mulls on a Bruker Vector 22 FTIR spectrometer.

Cyclic voltammetry measurements were performed by using a Wenking HP72 potentiostat, a Wenking VSG 72 signal generator, and a Graphext WX 2300 recorder. Measurements were conducted in a standard three-compartment cell with a platinum disk working electrode, platinum wire counter electrode, and  $\text{Ag}/\text{AgCl}$  (in aqueous tetramethylammonium chloride) reference electrode calibrated to SCE.

Photophysical measurements were made in 1,2-dichloroethane that was distilled from  $\text{CaH}_2$ . Corrected emission spectra, emission quantum yields, excited-state lifetimes, transient absorbance difference spectra, and ground- and excited-state resonance Raman spectra were measured as previously described.<sup>2,16–19</sup>

EPR spectra were recorded on a Bruker ECS 106 EPR spectrometer with an ESP 320 Data System. The sample was prepared by bulk electrolysis in situ and deoxygenated by sparging with argon for 10 min. The spectra were calibrated with DPPH ( $\alpha,\alpha'$ -diphenyl- $\beta$ -picrylhydrazyl). The EPR spectra were simulated by using a University of Rochester program.

Frontier molecular orbital (FMO) calculations and full geometry optimization for Aqphen were accomplished by using PM3 methods<sup>20</sup> implemented in the SPARTAN package.<sup>21</sup>

**Time-Resolved Infrared.** Time-resolved infrared measurements utilized a BioRad FTS 60A/896 step-scan interferometer with an external MCT detector as previously described.<sup>22,23</sup> A recent upgrade of this instrument utilizes fast data processing techniques. In this arrangement, the IR signal from the detector was amplified and processed by a BioRad Fast TRS board installed in a Pentium PC. This board also controlled the mirror movement, which operated at 10 Hz.

Individual points on the interferogram were collected every 200 ns after the laser pulse for 3  $\mu\text{s}$ . The data were organized into individual interferograms, representing the interferogram at every 200 ns point, then Fourier transformed into spectra. Spectra were averaged from immediately after the laser pulse to 1  $\mu\text{s}$  to give the final spectra. The

- (12) Klahn, A. H.; Oelckers, B.; Toro, A.; Godoy, F. *J. Organomet. Chem.* **1997**, *548*, 121.  
 (13) Chen, P.; Duesing, R.; Graff, D. K.; Meyer, T. J. *J. Phys. Chem.* **1991**, *95*, 5850–5858.  
 (14) Chen, P. Y.; Westmoreland, T. D.; Danielson, E.; Schanze, K. S.; Anthon, D.; Neveaux, P. E.; Meyer, T. J. *Inorg. Chem.* **1987**, *26*, 1116.  
 (15) Worl, L. A.; Duesing, R.; Chem, P.; Della Ciana, L.; Meyer, T. J. *J. Chem. Soc., Dalton Trans.* **1991**, 849–858.

- (16) Treadway, J. A.; Chen, P.; Rutherford, T. J.; Keene, F. R.; Meyer, T. J. *J. Phys. Chem. A.* **1997**, *101*, 6824–6826.  
 (17) Treadway, J. A.; Loeb, B. L.; Lopez, R.; Anderson, P. A.; Keene, F. R.; Meyer, T. J. *Inorg. Chem.* **1996**, *35*, 2242–2246.  
 (18) Strouse, G. F.; Schoonover, J. R.; Duesing, R.; Meyer, T. J. *Inorg. Chem.* **1995**, *34*, 2725–2734.  
 (19) Schoonover, J. R.; Strouse, G. F.; Chen, P.; Bates, W. D.; Meyer, T. J. *Inorg. Chem.* **1993**, *32*, 2618–2619.  
 (20) Lee, C.; Yang, W.; Parr, R. G. *Phys. Rev.* **1988**, *B37*, 785.  
 (21) SPARTAN, 4.1 ed.; Wave function Inc.: Irvine, CA, 1996.  
 (22) Omberg, K. M.; Schoonover, J. R.; Treadway, J. A.; Leasure, R. M.; Dyer, R. B.; Meyer, T. J. *J. Am. Chem. Soc.* **1997**, *119*, 7013–7018.  
 (23) Omberg, K. M.; Schoonover, J. R.; Meyer, T. J. *J. Phys. Chem.* **1997**, *101*, 9531.

**Table 1.** UV–Visible Absorption Maxima and  $E_{1/2}$  Values (vs SSCE with 0.1 M TBAH as Electrolyte) at 298 K

complex or compound	$\lambda_{\max}$ (nm)	$E_{1/2}(\text{Aqphen}^{0/+})$ (V)	$E_{1/2}(\text{oxidation})$ (V)	$E_{1/2}(\text{PTZ}^{0/+})$ (V)
Aqphen <sup>a</sup>	396, 410	−0.50, −0.80		
<i>fac</i> -[Re(Aqphen)(CO) <sub>3</sub> (Cl)] <sup>a</sup>	380, 403	−0.40, −0.86	+1.52	
<i>fac</i> -[Re(Aqphen)(CO) <sub>3</sub> (OTf)] <sup>a</sup>	380, 405	−0.22, −0.86	+1.63	
<i>fac</i> -[Re(Aqphen)(CO) <sub>3</sub> (4-Etpy)] <sup>+b</sup>	381, 404	−0.30, −0.86	+1.49	
<i>fac</i> -[Re(Aqphen)(CO) <sub>3</sub> (py-PTZ)] <sup>+b</sup>	383, 405	−0.28, −0.75	+1.62	+0.98
[Ru(bpy) <sub>2</sub> (dppz)] <sup>2+,a</sup>	356, 366, 442			
[Ru(bpy) <sub>2</sub> (Aqphen)] <sup>2+,a</sup>	380, 398, 446, 510	−0.22, −0.84	+1.28	

<sup>a</sup> In 1,2-dichloroethane as PF<sub>6</sub><sup>−</sup> salts. <sup>b</sup> In acetonitrile, as PF<sub>6</sub><sup>−</sup> salts.

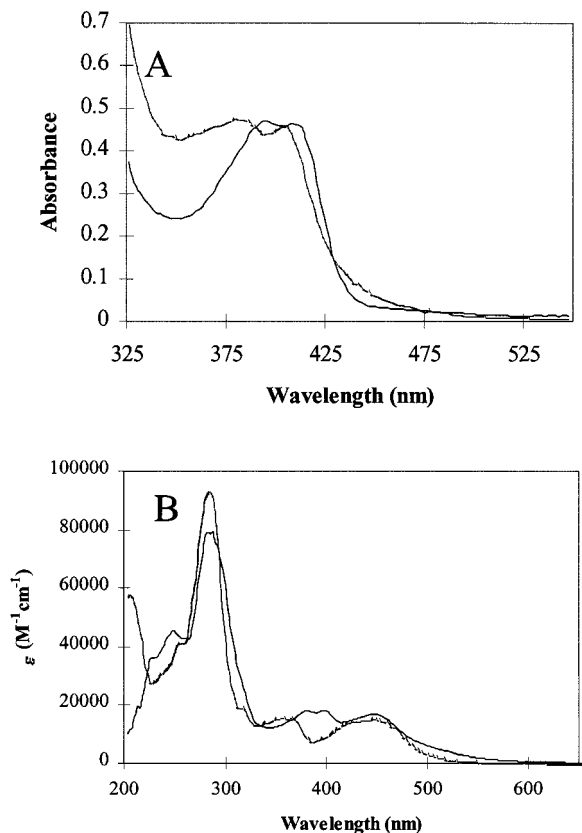


**Figure 1.** (A) UV–visible absorption spectra of Aqphen (—) and *fac*-[Re(Aqphen)(CO)<sub>3</sub>(py-PTZ)]<sup>+</sup> (---) in 1,2-dichloroethane and (B) [Ru(bpy)<sub>2</sub>(Aqphen)]<sup>2+</sup> (—) and [Ru(bpy)<sub>2</sub>(dppz)]<sup>2+</sup> (---) in 1,2-dichloroethane.

ground-state spectrum shown is an average of 64 scans, and the excited-state spectrum is an average of 128 scans.

TRIR spectra were measured in 1,2-dichloroethane or acetonitrile-*d*<sub>3</sub>, in a 1 mm path length sealed CaF<sub>2</sub> cell. Sample concentrations were adjusted to give an absorbance of ~0.7 for the  $\nu(\text{CO})$  bands. The sample cell and sample solutions were deoxygenated by sparging with argon for 15 min; solutions were transferred to the cell under an inert atmosphere. Spectra were acquired in blocks of 32 to prevent sample decomposition.

## Results

**Absorption Spectra.** The UV–visible absorption spectra of Aqphen and *fac*-[Re(Aqphen)(CO)<sub>3</sub>(py-PTZ)]<sup>+</sup> in 1,2-dichloroethane are shown in Figure 1A and of [Ru(bpy)<sub>2</sub>(Aqphen)]<sup>2+</sup> and [Ru(bpy)<sub>2</sub>(dppz)]<sup>2+</sup> in Figure 1B. The ligand spectrum is dominated by  $\pi \rightarrow \pi^*$  bands at 396 and 410 nm of roughly equal intensity ( $\epsilon \sim 15\,000 \text{ M}^{-1} \text{ cm}^{-1}$ ). These bands shift to a single convoluted absorption at 383 in *fac*-[Re(Aqphen)(CO)<sub>3</sub>(py-PTZ)]<sup>+</sup>. A  $\text{Re}^I \rightarrow \pi^*(\text{Aqphen})$  MLCT band appears at 405 nm. In [Ru(bpy)<sub>2</sub>(Aqphen)]<sup>2+</sup>, the ligand-based bands are also blue-shifted, appearing as separate components at 380 and 398

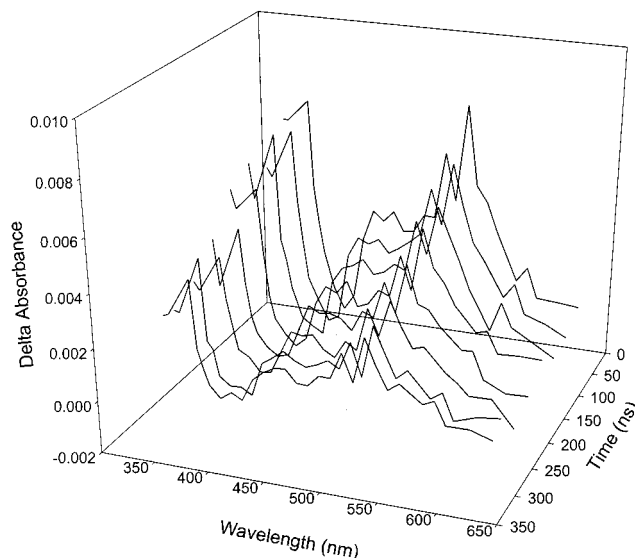


**Figure 2.** Transient absorption difference (TA) spectra for *fac*-[Re(Aqphen)(CO)<sub>3</sub>(py-PTZ)]<sup>+</sup> (laser flash excitation at 354.7 nm, 10 ns pulse width; in 1,2-dichloroethane) from 0 to 300 ns at 20 ns intervals.

nm. A broad MLCT band appears at 446 nm and a shoulder at 510 nm. In the spectrum of [Ru(bpy)<sub>2</sub>(dppz)]<sup>2+</sup>, ligand-based bands appear at 356 and 366 nm with a broad MLCT band at 449 nm. Spectral and electrochemical data are summarized in Table 1.

**Emission.** No emission was observed for *fac*-[Re(Aqphen)(CO)<sub>3</sub>(Cl)], *fac*-[Re(Aqphen)(CO)<sub>3</sub>(4-Etpy)]<sup>+</sup>, or *fac*-[Re(Aqphen)(CO)<sub>3</sub>(py-PTZ)]<sup>+</sup> in 1,2-dichloroethane at 298 or 77 K. *fac*-[Re(Aqphen)(CO)<sub>3</sub>(OTf)] displayed a very weak emission at 525 nm in 1,2-dichloroethane at 298 K with  $\tau < 20$  ns.

**Excited-State Spectra.** The transient absorbance difference (TA) spectrum of *fac*-[Re(Aqphen)(CO)<sub>3</sub>(py-PTZ)]<sup>+</sup> is shown in Figure 2 (laser flash excitation at 354.7 nm, 10 ns pulse width; in 1,2-dichloroethane at 298 K) at 20 ns time intervals from 20 to 300 ns. At 20 ns, new features are evident at 475, 510, and 560 nm, which decay with  $\tau = 300$  ns ( $k = 3.33 \times 10^6 \text{ s}^{-1}$ ), independent of monitoring wavelength. The feature at 560 nm is also present in the transient absorbance difference spectra of *fac*-[Re(Aqphen)(CO)<sub>3</sub>(OTf)] and *fac*-[Re(Aqphen)(CO)<sub>3</sub>(4-Etpy)]<sup>+</sup> following laser flash excitation at 354.7 nm (deconvoluted from the laser pulse since both lifetimes are  $< 20$  ns). It arises from a  $\pi \rightarrow \pi^*$  transition localized on the reduced Aqphen ligand and corresponds to a band that appears at 560 nm in the spectrum of electrochemically generated Aqphen<sup>•−</sup>.<sup>5</sup> Characteristic bands for PTZ<sup>•+</sup> are also present in the TA spectrum of *fac*-[Re(Aqphen)(CO)<sub>3</sub>(py-PTZ)]<sup>+</sup> at 475 and 510 nm.<sup>16,18,25–27</sup>

(24) Bates, W. D.; Bates, W. D., Ed.; University of North Carolina at Chapel Hill: Chapel Hill, 1995.

(25) Chen, P.; Mecklenburg, S. L.; Duesing, R.; Meyer, T. J. *J. Phys. Chem.* **1993**, *97*, 6811–6815.

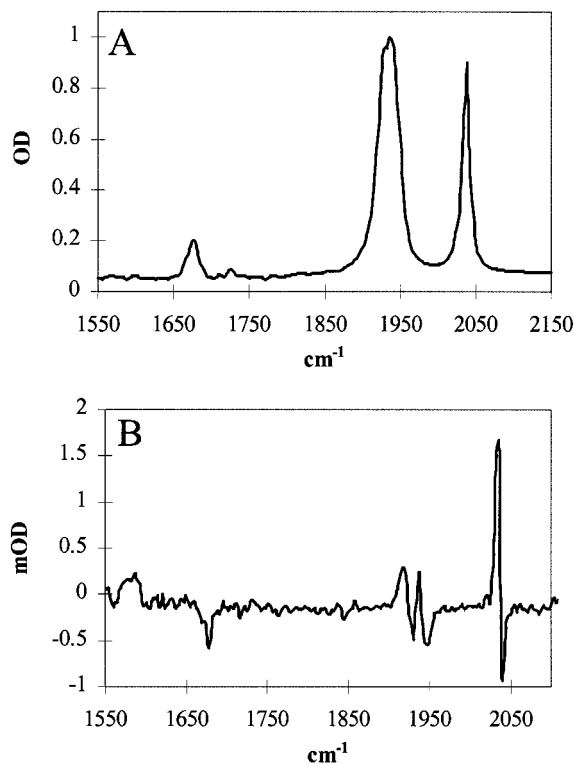


**Figure 3.** Ground-state (A) and TRIR absorption difference (B) spectra for *fac*-[Re(Aqphen)(CO)<sub>3</sub>(py-PTZ)]<sup>+</sup> between 1550 and 2100 cm<sup>-1</sup> in 1,2-dichloroethane at 298 K.

Ground-state and TRIR absorption difference spectra for *fac*-[Re(Aqphen)(CO)<sub>3</sub>(py-PTZ)]<sup>+</sup> between 1550 and 2100 cm<sup>-1</sup> in 1,2-dichloroethane at 298 K are shown in Figure 3. In the ground-state spectrum,  $\nu(\text{CO})$  bands appear at 2040, 1938, and 1932 cm<sup>-1</sup>, arising from the A'(1), A'(2), and A'' modes in pseudo-*C*<sub>3v</sub> symmetry. A quinone-based band appears at 1678 cm<sup>-1</sup>. The quinone vibration is a mixed mode, including both ring-stretching and C=O character.<sup>28</sup> In the TRIR difference spectrum, the  $\nu(\text{CO})$  bands are shifted to 2034, 1935, and 1917 cm<sup>-1</sup> and the quinone band to 1560 cm<sup>-1</sup>.

Time-resolved resonance Raman (TR<sup>3</sup>) band energies, relative intensities, and assignments for *fac*-[Re(Aqphen)(CO)<sub>3</sub>Cl] and *fac*-[Re(Aqphen)(CO)<sub>3</sub>(py-PTZ)]<sup>+</sup> in 1,2-dichloroethane at 298 K (354.7 nm excitation and scattering; ~4 mJ per pulse) are listed in Table 2. The spectrum is dominated by bands arising from the Aqphen ligand. These bands arise predominantly from the phenanthroline (phen) or phenazine parts of the ligand,<sup>2,29</sup> but the quinone-based band is also observed at 1675 cm<sup>-1</sup>.<sup>28</sup>

**EPR.** The EPR spectrum of once-reduced Aqphen<sup>•-</sup> generated by reduction with potassium *t*-butoxide in DMSO is shown in Figure 4A. The hyperfine splitting corresponds to a quinone-based reduction with the unpaired electron interacting with one hydrogen (H8, based on the numbering scheme in Figure 4A) and two pairs of two equivalent hydrogens (H9 and H12). The simulated spectrum is shown in the insert. Simulation of the spectrum gave  $a_{\text{H}} = 0.51$  mT,  $a_{2\text{H}} = 0.15$  mT, and  $a_{2\text{H}} = 0.21$

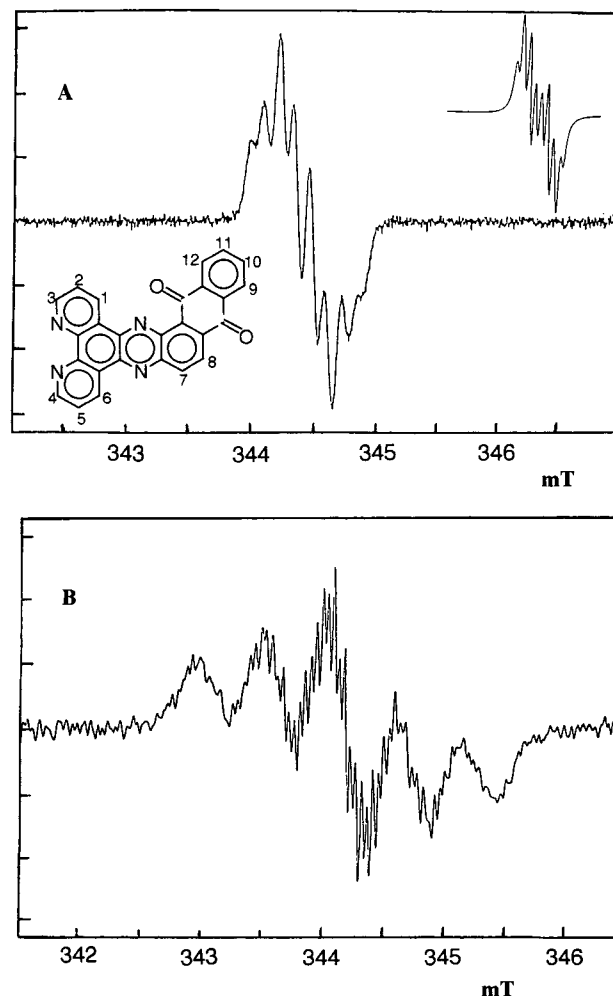


**Figure 4.** (A) EPR spectrum of once-reduced Aqphen<sup>•-</sup> generated by reduction with potassium *t*-butoxide in DMSO. The simulated spectrum and numbering scheme are shown in the insert. (B) EPR spectrum of once-reduced dppz<sup>•-</sup> generated by reduction with potassium *t*-butoxide in DMSO.

**Table 2.** TR<sup>3</sup> Band Energies (in cm<sup>-1</sup>; 354.7 nm excitation and scattering, ~4 MJ per pulse), Relative Intensities,<sup>a</sup> and Assignments for *fac*-[Re(Aqphen)(CO)<sub>3</sub>Cl] and *fac*-[Re(Aqphen)(CO)<sub>3</sub>(py-PTZ)]<sup>+</sup> in 1,2-Dichloroethane at 298 K

<i>fac</i> -[Re(Aqphen)(CO) <sub>3</sub> (py-PTZ)] <sup>+</sup>	<i>fac</i> -[Re(Aqphen)(CO) <sub>3</sub> Cl]	assignment
1160w	1160 w	phenazine
1174 m	1174 m	coupled phen + phenazine
1291 s	1291 s	phen
	1319 w	phen
	1347 w	phen
1404 s	1404 s	phenazine
	1467 s	phenazine
	1545 m	phen
	1578 m	phen
	1596 m	phen
1675 w	1675 w	anthraquinone

<sup>a</sup> s = strong; m = medium; w = weak.

mT. The EPR spectrum of once-reduced dppz<sup>•-</sup> is shown in Figure 4B for comparison. The five-line pattern observed in this spectrum is significantly different from the pattern for Aqphen<sup>•-</sup>, consistent with interaction between the added electron and two equivalent nitrogen atoms on the phenazine portion of the ligand with a coupling constant of 0.56 mT.

**Molecular Orbital Calculations.** The orbital coefficients for the HOMO and first three LUMO levels for Aqphen and the

(26) Shover, R. J.; Perkovic, M. W.; Rillema, D. P.; Woods, C. *Inorg. Chem.* **1995**, *34*, 6421.

(27) Duesing, R.; Tapolsky, G.; Meyer, T. J. *J. Am. Chem. Soc.* **1990**, *112*, 5378.

(28) Burie, J.-R.; Boussac, A.; Boullais, C.; Berger, G.; Mattioli, T.; Mioskowski, C.; Nabedryk, E.; Breton, J. J. *Phys. Chem.* **1995**, *99*, 4059.

(29) Bates, W. D.; Chen, P.; Bignozzi, C. A.; Schoonover, J. R.; Meyer, T. J. *Inorg. Chem.* **1995**, *34*, 6215–6217.



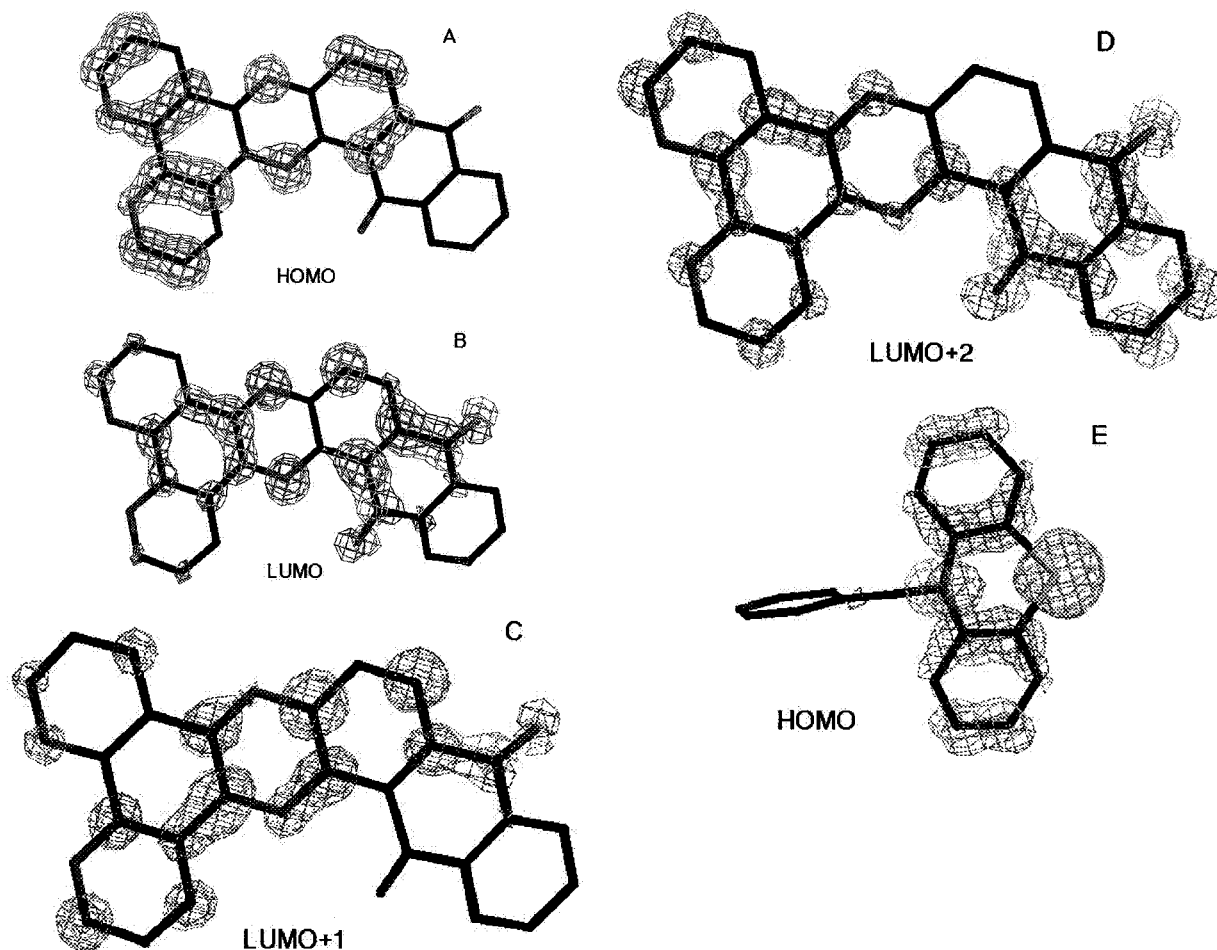


**Figure 5.** Illustrations of electronic distributions for the HOMO (A) and first three LUMO (B, C, D) levels for Aqphen and the HOMO for py-PTZ (E) calculated with frontier molecular orbital calculations and full geometry optimization by using PM3 methods<sup>20</sup> implemented in the SPARTAN software package.<sup>21</sup>

HOMO for py-PTZ were calculated by using the FMO method with full geometry optimization by using PM3 methods<sup>20</sup> implemented in the SPARTAN software package.<sup>21</sup> The results are illustrated in Figure 5. They show that the Aqphen-based HOMO is largely centered in the phen and phenazine portions of the ligand with considerable N 2p character for the N atoms bound to  $\text{Re}^{\text{I}}$ . In contrast, the first Aqphen-based LUMO is largely centered on the quinoid portion of the ligand with nodes at the coordinating N atoms. The ring framework of the Aqphen ligand is slightly bent at the quinoid C=O, with  $\angle\text{C}-\text{C}(\text{O})-\text{C} = 32^\circ$ . In py-PTZ, the HOMO is largely centered on the phenothiazine, with no significant contribution from pyridine.

## Discussion

**Ground-State Spectra.** In UV-visible spectra of  $\text{Ru}^{\text{II}}$  dppz complexes, separate MLCT bands have been observed for transitions to  $\pi^*$  levels localized largely on the phenazine and phenanthroline portions of the ligands with the energy ordering  $\pi_1^*(\text{phenazine}) < \pi_2^*(\text{phenanthroline})$ .<sup>19,24</sup> In  $[\text{Ru}(\text{bpy})_2(\text{dppz})]^{2+}$ , an MLCT band arising from overlapping  $\text{Ru}^{\text{II}} \rightarrow \pi^*(\text{bpy})$  and  $\text{Ru}^{\text{II}} \rightarrow \pi^*(\text{phenazine})$  transitions is observed at  $\sim 485$  nm with  $\text{Ru}^{\text{II}} \rightarrow \pi^*(\text{phenanthroline})$  appearing at  $\sim 450$  nm; the latter as shown by low-temperature measurements.<sup>24</sup> For  $[\text{Ru}(\text{bpy})_2(\text{Aqphen})]^{2+}$ , overlapping  $\text{Ru}^{\text{II}} \rightarrow \pi^*(\text{bpy})$  and  $\text{Ru}^{\text{II}} \rightarrow \pi^*(\text{phenanthroline})$  bands appear at 446 nm, and  $\text{Ru}^{\text{II}} \rightarrow \pi^*(\text{phenazine})$  appears as a shoulder at 510 nm (Figure 1B,  $\epsilon \approx 1000 \text{ M}^{-1} \text{ cm}^{-1}$ ). In the spectrum of  $\text{fac}[\text{Re}(\text{Aqphen})(\text{CO})_3(\text{py-PTZ})]^+$ , there is no evidence for separate  $\text{Re}^{\text{I}} \rightarrow \pi^*$

(phenanthroline) and  $\text{Re}^{\text{I}} \rightarrow \pi^*(\text{phenazine})$  bands in the broad MLCT manifold centered at 405 nm.

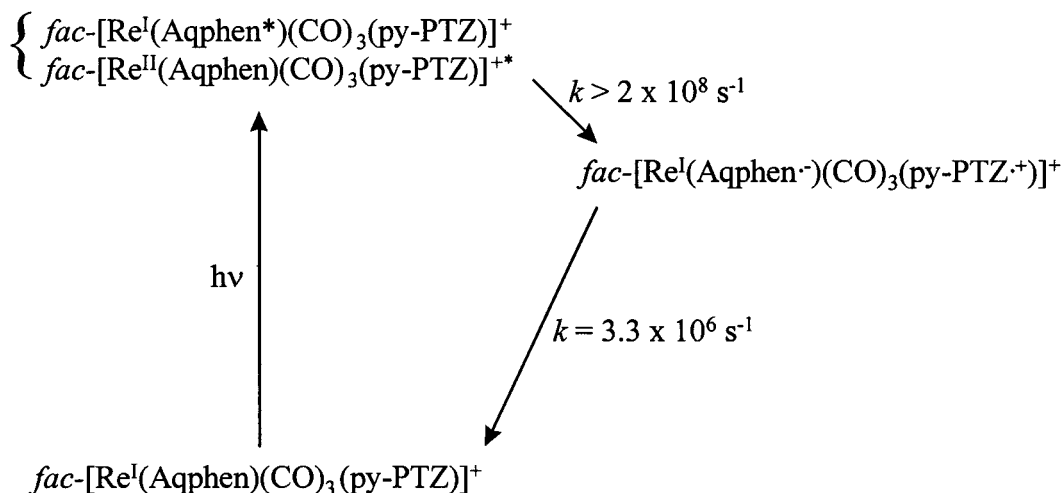
Aqphen is structurally related to dppz but includes the appended quinone acceptor. The absorption feature at 510 nm in the spectrum of  $[\text{Ru}(\text{bpy})_2(\text{Aqphen})]^{2+}$  has a significant tail extending past 600 nm, but we have been unable to find direct evidence for a  $\text{Ru}^{\text{II}} \rightarrow \pi^*(\text{quinone})$  band at lower energy, even at high concentrations ( $\sim 10$  mM). If such a band exists,  $\epsilon < 100 \text{ M}^{-1} \text{ cm}^{-1}$ .

The absence of discernible intensity for this band is consistent with the results of the FMO calculations. They show that the LUMO is largely quinone-based with no significant contribution from  $2p_\pi$  at the coordinated N atoms (Figure 5). It is also consistent with the EPR spectrum and the absence of nitrogen hyperfine splitting in the reduced ligand, which points to a high degree of localization on the quinone fragment in the LUMO.

On the basis of the combined spectral and electrochemical data, three  $\pi^*$  acceptor levels play a role in the spectral and redox properties of the Aqphen ligand, with the energy ordering:  $\pi_1^*(\text{quinone}) < \pi_2^*(\text{phenazine}) < \pi_3^*(\text{phenanthroline})$ .

**Excited-State Spectra.** Laser flash excitation of  $\text{fac}[\text{Re}(\text{Aqphen})(\text{CO})_3(\text{py-PTZ})]^+$  at 354.7 nm in 1,2-dichloroethane results in the appearance of a transient with characteristic features for  $\text{PTZ}^{\bullet+}$  at 475 and 510 nm. An additional Aqphen $^{\bullet-}$ -based feature appears at 560 nm, as a broadening of the  $\text{PTZ}^{\bullet+}$  band at 510 nm. The appearance of these features is consistent with formation of the redox-separated state,  $\text{fac}[\text{Re}^{\text{I}}(\text{Aqphen}^{\bullet-})-$

Scheme 1



(CO)<sub>3</sub>(py-PTZ<sup>•+</sup>)<sup>+</sup>. This transient is formed within the laser pulse and decays with  $\tau_{298\text{K}} = 300 \text{ ns}$  ( $k = 3.33 \times 10^6 \text{ s}^{-1}$ ), independent of monitoring wavelength from 450 to 600 nm.

The overlap of PTZ<sup>•+</sup> and Aqphen<sup>•-</sup> absorptions in the transient absorption difference spectrum leaves the question of detailed electronic distribution somewhat ambiguous in the photochemical transient. This ambiguity is removed by the TRIR absorption difference spectrum in Figure 3. Four new bands appear for the transient between 1550 and 2100 cm<sup>-1</sup> (Figure 3). The three  $\nu(\text{CO})$  bands in the ground state are shifted by only -6, -3, and -15 cm<sup>-1</sup>, to 2034, 1935, and 1917 cm<sup>-1</sup>. Ground-to-excited state shifts for MLCT excited states are typically much larger and in the opposite direction (for *fac*-[Re<sup>II</sup>(bpy<sup>•-</sup>)(CO)<sub>3</sub>(4-Etpy)]<sup>+</sup>, the shifts are +25, +80, and +35 cm<sup>-1</sup> in CH<sub>3</sub>CN at 298 K).<sup>23</sup> The small shifts in the photochemical transient show that the electron density at the metal is relatively unperturbed compared to the ground state.<sup>30-33</sup>

The quinone-based CO stretch shifts from 1678 cm<sup>-1</sup> in the ground state to 1560 cm<sup>-1</sup> in the transient. This shift of 118 cm<sup>-1</sup> is comparable to those of the once-reduced complex (131 cm<sup>-1</sup>) and fully reduced Aqphen<sup>•-</sup> (126 cm<sup>-1</sup>) generated electrochemically or fully reduced naphthoquinone (122 cm<sup>-1</sup>),<sup>28</sup> which is consistent with essentially complete reduction at the quinone. This conclusion is also consistent with the EPR results and the FMO calculations, which show that the LUMO is predominantly localized on the quinone portion of the ligand with some contribution from the phenazine portion and little contribution from the phen portion.

The appearance of new absorption features at 475 and 510 nm provide evidence for the presence of PTZ<sup>•+</sup> in the transient. On the basis of the results of the FMO calculations, oxidation is localized largely on the phenothiazine, electronically isolated from the bridging pyridine. This is also consistent with the small shifts in  $\nu(\text{CO})$  which show that there is no significant electronic interaction between Re<sup>I</sup> and PTZ<sup>•+</sup> in the transient.

The spectroscopic data on the transient clearly demonstrate that it is the redox-separated state *fac*-[Re<sup>I</sup>(Aqphen<sup>•-</sup>)(CO)<sub>3</sub>(py-PTZ<sup>•+</sup>)]<sup>+</sup> with the oxidative and reductive equivalents largely localized on PTZ and Aqphen, respectively, and with weak electronic coupling between them.

There are clear similarities between the TR<sup>3</sup> spectra of *fac*-[Re(Aqphen)(CO)<sub>3</sub>(py-PTZ)]<sup>+</sup> and *fac*-[Re(Aqphen)(CO)<sub>3</sub>(Cl)] (Table 2), notably in the exact coincidence of bands arising from the phenazine portion of the ligand at 1160, 1174, and 1404 cm<sup>-1</sup>, a phenanthroline-based band at 1291 cm<sup>-1</sup>, and the quinone-based band at 1675 cm<sup>-1</sup>. Given the excitation and scattering wavelength of 354.7 nm, the resonance enhancements most likely arise from a  $\pi \rightarrow \pi^*$  transition localized on the quinone radical anion in Aqphen<sup>•-</sup>. Since the TR<sup>3</sup> experiment probes the lowest-lying electronic excited state, this is an important comparison suggesting that the electronic distribution in the acceptor ligand in the "MLCT" excited state, *fac*-[Re<sup>II</sup>(Aqphen<sup>•-</sup>)(CO)<sub>3</sub>(Cl)], is similar to that in the redox-separated state, *fac*-[Re<sup>I</sup>(Aqphen<sup>•-</sup>)(CO)<sub>3</sub>(py-PTZ<sup>•+</sup>)]<sup>+</sup>. In this interpretation, a more appropriate description of this state is that it is a redox-separated state with weak to moderate electronic coupling between Re<sup>II</sup> and Aqphen<sup>•-</sup>.

The only significant difference between the time-resolved resonance Raman (TR<sup>3</sup>) spectra of these two transients is that additional phen-based bands appear at 1319, 1347, 1545, 1578, and 1596 cm<sup>-1</sup> for *fac*-[Re<sup>II</sup>(Aqphen<sup>•-</sup>)(CO)<sub>3</sub>(Cl)]. This is because the two are different electronically. In *fac*-[Re<sup>II</sup>(Aqphen<sup>•-</sup>)(CO)<sub>3</sub>(Cl)], the phen portion of the ligand is bound to Re<sup>II</sup>. In *fac*-[Re<sup>I</sup>(Aqphen<sup>•-</sup>)(CO)<sub>3</sub>(py-PTZ<sup>•+</sup>)]<sup>+</sup>, it is bound to Re<sup>I</sup>. Since resonance enhancement is proportional to distortion, the appearance of additional coupled modes for the excited state is expected. In *fac*-[Re<sup>I</sup>(Aqphen<sup>•-</sup>)(CO)<sub>3</sub>(py-PTZ<sup>•+</sup>)]<sup>+</sup>, there is little distortion along the Re<sup>II</sup>-N bonds and little distortion in the phen-based vibrational modes. In *fac*-[Re<sup>II</sup>(Aqphen<sup>•-</sup>)(CO)<sub>3</sub>(Cl)], there is more distortion along the Re<sup>II</sup>-N bonds and more distortion in the phen-based modes.

There are no resonantly enhanced quinone-based bands in either TR<sup>3</sup> spectrum. The resonance enhancement is due to a  $\pi \rightarrow \pi^*(\text{Aqphen}^{\bullet-})$  transition, and the quinone-based modes are only weakly coupled to the transition.

**Kinetic Scheme.** The observations discussed in the previous section are consistent with the sequence of events in Scheme 1, in which Re<sup>I</sup>  $\rightarrow \pi^*(\text{Aqphen})$ ,  $\pi \rightarrow \pi^*(\text{Aqphen})$  excitation at 354.7 nm is followed by rapid (<10 ns) intramolecular electron transfer (PTZ  $\rightarrow$  Re<sup>II</sup>, PTZ  $\rightarrow \pi$ ) to give the observed transient.

Back electron transfer between Aqphen<sup>•-</sup> and PTZ<sup>•+</sup> in Scheme 1 occurs with  $k_{298\text{K, DCE}} = 3.3 \times 10^6 \text{ s}^{-1}$  and  $\Delta G^\circ = -1.04 \text{ eV}$ , based on the electrochemical measurements. Given the magnitude of the driving force, back electron transfer is remarkably slow, at least compared with rate constants for back electron transfer in the related series *fac*-[Re<sup>I</sup>(4,4'-(X)<sub>2</sub>bpy<sup>•-</sup>)(CO)<sub>3</sub>(py-PTZ<sup>•+</sup>)]<sup>+</sup>.<sup>13</sup> In that series, back electron transfer in

(30) Schoonover, J. R.; Strouse, G. F.; Omberg, K. M.; Dyer, R. B. *Comments Inorg. Chem.* **1996**, *18*, 165.

(31) Schoonover, J. R.; Bignozzi, C. A.; Meyer, T. J. *Coord. Chem. Rev.* **1997**, *165*, 239-266.

(32) Turner, J. J.; George, M. W.; Johnson, F. P. A.; Westwell, J. R. *Coord. Chem. Rev.* **1993**, *125*, 101.

(33) Glyn, P.; George, M. W.; Hodges, P. M.; Turner, J. J. *J. Chem. Soc., Chem. Commun.* **1989**, 1655.

*fac*-[Re<sup>I</sup>(4,4'-(CO<sub>2</sub>Et)<sub>2</sub>bpy<sup>•-</sup>)(CO)<sub>3</sub>(py-PTZ<sup>•+</sup>)]<sup>+</sup> occurs with  $k_{298\text{K, DCE}} = 4.0 \times 10^7 \text{ s}^{-1}$  with  $\Delta G^\circ = -1.36 \text{ eV}$ . These reactions occur in the inverted region with  $\ln(k)$  increasing with decreasing  $-\Delta G^\circ$ . The slow rate of back electron transfer for *fac*-[Re<sup>I</sup>(Aqphen<sup>•-</sup>)(CO)<sub>3</sub>(py-PTZ<sup>•+</sup>)]<sup>+</sup> is likely a consequence of weak electronic coupling between the Aqphen<sup>•-</sup> donor and the PTZ<sup>•+</sup> acceptor. The oxidative equivalent is localized on the PTZ part of py-PTZ and the reductive equivalent on the quinone in a  $\pi^*$  orbital with nodes at the metal.

**Acknowledgment.** Financial support from Fondecyt-Chile (Grants 1940577 and 1971202 to B.L.), Conicyt-Chile (Grant

2950063 to R.L.), and the National Science Foundation (Grant CHE-9705724 to T.J.M.) is gratefully acknowledged. Travel between the laboratories at PUC and UNC (R.L., B.L.) was supported by the National Science Foundation and Conicyt (Grant INT-9704277). This work was performed in part at Los Alamos National Laboratory under the auspices of the U.S. Department of Energy and was supported by funds provided by the University of California for the conduct of discretionary research by Los Alamos to J.R.S.

IC981050W